Langmuir

Article

pubs.acs.org/Langmuir

Dispersions of Monodisperse Hybrid Rod-Like Particles by Mineralization of Filamentous Viruses

Emilie Pouget† and Eric Grelet*

Centre de Recherche Paul-Pascal, CNRS & Université de Bordeaux, 115 Avenue Schweitzer, F-33600 Pessac, France

Supporting Information

ABSTRACT: In this work, we report on the synthesis through a direct chemical approach of hybrid organic/inorganic rod-like particles with a very high aspect ratio (length/diameter) by the use of a biotemplate, the fd virus. A synthetic route is proposed based on an initial step of steric stabilization of the colloidal template by hydrophilic polymer grafting. Thanks to this polymer functionalization, the filamentous viruses are well-dispersed in solution during their mineralization by different inorganic salts, leading to suspensions of individual hybrid rod-like particles such as virus/SiO_2 and virus/TiO_2. This aqueous solution based approach is shown to be highly reproducible, scalable for large production synthesis, and versatile to different inorganic materials.

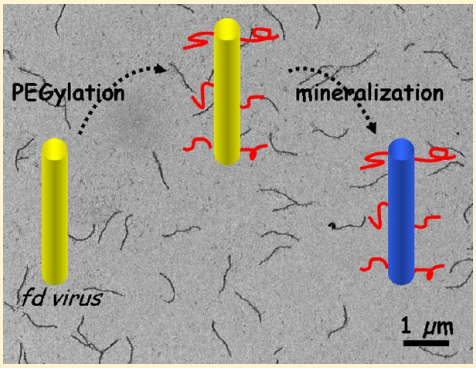

INTRODUCTION

For at least two decades, synthesis, study, and use of inorganic nano-objects have known a real development.[1−3] More and more complex materials are created on the nanoscale such as spheres,[4] rods,[5,6] tubes,[3,7] platelets,[8,9] twisted ribbons, and helices.[10] Depending on their chemical compositions, these inorganic nanostructures cover a very large domain of applications including electronics, optics, sensing, etc.[1] If spherical nanoparticles are easily formed by complexation in solution,[4] anisotropic inorganic objects such as tubes or rods are more difficult to create, despite their great interest steming from the magnification of their properties in the direction of anisotropy. Moreover, their self-organization is also richer and more varied than isotropic particles, with the appearance for instance of liquid crystalline phases. The self-assembly into a set of mesophases is a way of hierarchical structuration which is one of the most challenging points in the nanoscience research nowadays.[11,12]

In a recent review, Xia et al.[1] summarized different methods to achieve unidimensional nanostructures based on bottom-up approaches. The main involved processes are the confinement, the self-assembly of spherical nanoparticles, the control by capping agents, or the crystallographic inhibition during the particle growth. In this last case, such a strategy is commonly used for ab initio synthesis of nanorods.[13] The use of organic self-assemblies as a template for the deposition of a mineral layer represents another widely explored approach for achieving various and complex morphologies such as tubes, sponges, etc.[1−3] Some of the templates frequently used are self-assembled surfactants, polymers, or peptides. These structures generally exhibit a very good monodispersity in diameter, but the tube or rod length is hardly monitored.[1−3] Only biological structures such as proteins or viruses exhibit high uniformity in sizes and shapes because their morphologies are genetically coded.[14,15] This intrinsic monodispersity provides them with a unique feature such as promising templates to generate well-defined and morphologically controlled hybrid structures. For this purpose, after the seminal work of Shenton et al. in 1999 where tobacco mosaic virus (TMV) was covered with different materials,[5] various studies have been published on the mineralization of filamentous viruses (mainly TMV and fd/M13 bacteriophages which are two close mutants).[16−22] Most of these works show the difficulty of the reproducibility of the mineralization process and the problem of aggregation of the particles during the chemical reactions. Different studies focused on the silicification of the TMV and fd viruses, but aggregation always occurred during the process inducing the formation of macroscopic fibers, bundles, or mesostructures.[17−19,23] Because of the difficulty of having a selective mineral deposition on individual viruses, an interesting work has been performed on the M13 virus with the use of genetic modifications (phage display technique) to express peptides having a specific affinity for an inorganic target material. In this way, Belcher's group has produced well-defined hybrid rod-like nanoparticles of silver, gold or zinc sulfate but only in limited amounts, for which no concentrated self-organized dispersions of these hybrid elongated particles have ever been reported.[20−22]

In the present work, we propose a novel strategy to synthesize large amounts of hybrid virus/mineral rod-like particles with high aspect ratio, weak polydispersity in size, and high colloidal stability. If these three characteristics have been

Received: March 27, 2013
Revised: May 27, 2013
Published: May 28, 2013

   dx.doi.org/10.1021/la401170m | Langmuir 2013, 29, 8010−8016

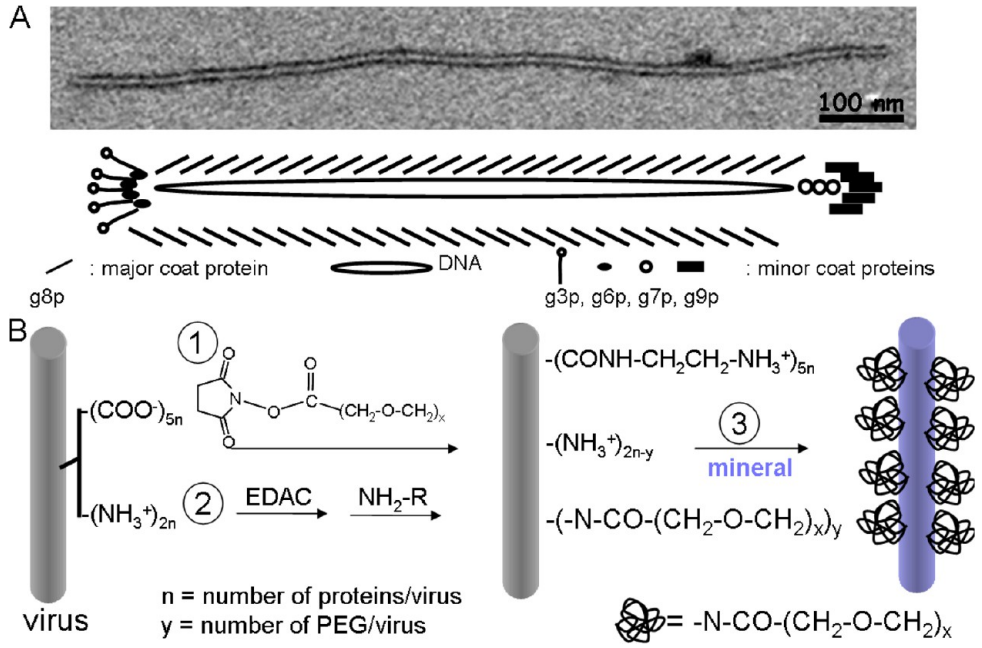

Figure 1. (A) Transmission electron microscopy (TEM) image of a negatively stained fd virus and its corresponding schematic structure. (B) Strategy of the synthesis developed in this work: the virus is schematically represented by a rigid rod and only the charged head groups of one among the n = 2700 copies of the major coat protein (g8p) are represented. (1) PEG-grafting, (2) inversion of the viral surfacic charge (EDAC is 1-ethyl-3-(3-dimethylaminopropyl)carbodiimide hydrochloride and R = CH_2−CH_2−NH_3^+), and (3) mineralization occurring at pH 6.

achieved separately,[17,24] no system of hybrid rod-like particles are known to exhibit simultaneously such an aspect ratio (L/D > 50), a low polydispersity in length (σ_L <4%) and diameter (σ_L <30%), and a large production scale (see the Supporting Information (SI)). In order to prevent the aggregation during the template mineralization, the viruses are first sterically stabilized by grafting hydrophilic polymers on their surface, allowing for their good dispersion in aqueous solution during the chemical reactions. In a second step, the surfacic charge of the viruses which is negative at physiological pH is reversed to positive in order to favor electrostatic attraction with the negatively charged mineral precursor salts. The virus template thus exhibits a high colloidal stability with a suitable surface for catalyzing the mineralization reaction. The general feature of this approach is demonstrated with the use of two kinds of minerals: silica and titanium dioxide.

The synthesis developed in this article is schematically depicted in Figure 1. The fd virus is a rod-like bacteriophage with a contour length of 880 nm, a diameter of 6.6 nm, and a persistence length of 2.8 μm, which can be produced in large amounts using standard biological protocols.[25] As shown in Figure 1A, each virus consists of a single strand DNA molecule packed in a cylindrical capsid composed of 2700 identical major coat proteins (g8p) and a few copies of four different minor coat proteins that cap each end.[26,27] The solvent-exposed part of the g8p contains seven charged amino-acids: two amino groups (Lys8 and N-terminus) and five acidic residues (Glu2, Asp4, Asp5, Asp12, and Glu20) which actively participate to the surface properties of the virus. It results a net electrical charge density of about 3 e^-/protein at physiological pH and the isoelectric point pI_E is 4.2. That is the reason why the fd viruses form, in aqueous solution, a stable colloidal suspension thanks to the electrostatic repulsions at physiological pH. While mineralizing the virus, an electrostatic neutralization of the system occurs and a strong aggregation appears due to van der Waals attraction between neutral particles. All of the attempts of mineralization of the fd virus with SiO_2 formed bundles, fibers, or nonorganized aggregates.[17,18,23] In the present work, the fd viruses are previously sterically stabilized by covalently grafting at the surface polyethylene glycol (PEG) with a molecular weight of 20 000 g/mol. A PEG prefunctionalized with a succinimidyle ester (NHS-PEG) is used to react with the amino groups (NH_2 terminal or lysine) of the major coat protein and create covalent bonds. An amount of 150 PEG/virus as evaluated by refractive index increment measurement was coated in order to induce the steric stability. This represents of about 5% of the main coat proteins for the polymer grafting, meaning that 95% of the coat proteins are still available for mineralization. This concentration is chosen to be low enough to keep a free access at the g8p surfacic head groups for the mineralization reaction while inducing the steric repulsion between viral particles (Figure 1B-1). Beside the general acidic surface, the amino groups are still present and should catalyze the condensation of the mineral salts. Unfortunately, the repulsion induced by the acidic residues on the silica precursors is strong enough to inhibit this reaction. In a previous work, Zhang et al. have obtained well-defined viruses that are permanently positively charged and are structurally stable over a wide range of pH.[28] A water-soluble carbodiimide was used to activate the carboxyl groups. The resulting O-acylisourea then reacts with the amino compounds, here the ethylenediamine (EDA), which has a positively charged group as well as a nucleophilic primary amino group that can react with the activated carboxyl group. One positive charge is then introduced while one negatively charged carboxyl group is transformed into a neutral amide bond (Figure 1B-2). In this way, the surface charge of fd becomes positive over a wide pH range without losing its structural integrity. The details of the different chemical reactions of the process are

dx.doi.org/10.1021/la401170m | Langmuir 2013, 29, 8010−8016

given in the experimental part and in the Supporting Information of this article.

The last synthetic step is the mineralization of the fd surface (Figure 1B-3), grafted with PEG polymers and positively charged at physiological pH (i.e., pH of the distilled water around 6). For the silica deposition, a prehydrolyzed tetra(ethyl-orthosilicate) (TEOS) solution is used. At the working pH, the surfacic amino groups catalyze the silica polymerization.[29,30] According to the Gouy−Chapman theory, the concentration of silica precursors R_3SiO^- or $(OH)_3SiO^-$ in the vicinity of the positively charged virus surface is much higher than in bulk solution.[31,7] This will ensure the special selectivity of the template surface and locally accelerates the silica condensation. Because most of the coat proteins (>95%) containing charged amines are available for mineralization, the diffusion of the molecular silica precursors through the polymers is possible and the condensation occurs at the surface of the virus. Consequently, we expect to keep the polymer chains free of mineralization to maintain the sterical stability of the final hybrid rod-like particles. For the titanium dioxide deposition, the sol−gel chemistry from alkoxides is well-known but is particularly fast and performed in extreme pH conditions or in ethanol.[32] Because of the biological nature of our template, the reaction of mineralization has to be held in soft conditions, i.e., in water and at a pH close to 7. A few years ago, a bioinspired approach was reported for the synthesis of TiO_2 by using a water-soluble precursor, titanium(IV) bis (ammonium lactate) dihydroxide (TiBALDH).[33] This non toxic and biodegradable precursor is chemically stable in water because of the remarkable retardation of hydrolysis for this chelate-type complex. Such a behavior is explained by the concepts of mean electronegativity of a given chemical species and partial charges of the element; that is, the hydrolysis is active until the mean electronegativity becomes equal to the mean electronegativity of water.[34] In TiBALDH, the complexation of Ti with the ligands decreases considerably the electronegativity of the complex and therefore the hydrolysis kinetics. The chemistry of this salt is still misunderstood but it has been shown that, in analogy with the silica condensation, proteins like silicateins or silafins catalyze the condensation of this precursor, forming hybrid organic/TiO_2 structures at room temperature.[33,35−37] More generally, all of the amine groups seem to catalyze the TiBALDH condensation.[38−43] The TiO_2 formed in these conditions is generally amorphous but some example of anatase or rutile obtained at room temperature has been published.[36] The TiO_2 crystallinity can also be induced by thermal annealing of the samples.[40,41]

EXPERIMENTAL SECTION

Chemicals. The succinimidyl ester polyethylene glycol (NHS-PEG 20 000 g/mol) was purchased from NOF Corporation, Japan (ref Sunbright ME-200HS). 1-Ethyl-3-(3-dimethylaminopropyl)-carbodiimide hydrochloride (EDAC), ethylenediamine (EDA), tetra(ethyl orthosilicate) (TEOS), and titanium(IV) bis (ammonium lactate) dihydroxide (TiBALDH) were purchased from Sigma-Aldrich and used without any further purification.

fd Virus Production. According to standard biological protocols, wild type fd bacterio-viruses were grown from *Escherichia coli* (*E. coli*) XL1-Blue strain as the bacterial host.[25] In this way, large amounts (tens of mg) of viruses were obtained. The viruses were then purified by sequential steps of centrifugation and ultracentrifugation. The concentration of the virus suspensions was determined using absorption spectroscopy with an optical density (OD) for a 1 mg/mL (6.1×10^{-8} M) virus solution of $OD_{269nm}^{10mm} = 3.84$.

Polymer Grafting. To graft polyethylene glycol to the amino groups of the coat proteins, the method reported in reference[44] was applied with some minor changes. A variable amount of NHS-PEG 20 000 g/mol was added under stirring to 10 mL of a virus dispersion at 1 mg/mL in 300 mM sodium phosphate buffer at pH 7.8. The grafting reaction was left standing for a few hours. To remove the residual polymers, a dialysis against distilled water (membranes MWCO 10 000 Da) was first performed, before two cycles of ultracentrifugation at 200 000*g* for 3 h followed each time by the redispersion of the pellet in distilled water. The amount of PEG grafted at the surface of the viruses were determined by refractive index increment technique. Hereafter, we refer to the resulting PEG-grafted fd virus as fd-PEG.

Modification of the Surfacic Carboxyl Groups of the fd Virus. For the chemical modification of the g8p proteins, the water-soluble carbodiimide, 1-ethyl-3-(3-dimethylaminopropyl)carbodiimide hydrochloride (EDAC), was used to activate the five carboxyl groups of Glu2, Asp4, Asp5, Asp12, and Glu20 of each coat protein exposed to the solvent. The resulting O-acylisourea then reacts with the ethylenediamine (EDA) which has a positively charged group as well as a nucleophilic primary amino group that can react with the activated carboxyl group. One positive charge is then introduced while one negatively charged carboxyl group is transformed into a neutral amide bond, resulting in an inversion (from negative to positive) of the virus charge at neutral pH (see the SI).[28]

A 10 mL solution of fd-PEG particles in distilled water was used at the concentration of 0.08 mg/mL (4.9×10^{-9} M) which corresponds to the nonoverlapping concentration of the rods in solution. Two aqueous solutions of 5 mL of EDA at 400 mM and 5 mL of EDAC at 320 mM were prepared. These two solutions represent a large excess of reactive species. The pH of both solutions was adjusted at 5−5.5 with 1 M HCl. The procedure is the following: under vigorous stirring, the EDA solution was added in the fd-PEG solution. Then half of the EDAC solution was added. After 3 h of stirring, the second half of the EDAC solution was added and the reaction occurred under magnetic stirring for 12 h at room temperature. The final dispersion was dialyzed against distilled water to remove residual amines and other byproducts.

In this paper, we refer to the resulting PEG-grafted viruses with an inversed surfacic charge as fd-PEG-CR.

It could have been envisaged to exchange the order of the process steps (1/surfacic charge inversion and 2/PEGylation), but in this last case, the PEG concentration at the surface of the viruses would have been radically increased because of the increase of the binding sites (amino groups), and it will be demonstrated later in this paper that the amount of PEG grafted on viruses plays a crucial role in the mineralization process.

Mineralization with SiO_2. The precursor used is the tetra(ethyl-orthosilicate), TEOS. The TEOS was prehydrolyzed before used: 15 v/v% of TEOS were mixed with water and stirred one night. Only the aqueous part of the solution is used for the experiments and the excess of TEOS is thrown away. According to the literature the concentration of silicic acid ($Si(OH)_4$) in water at pH 6 is around 10^{-3} M and the concentration of other potential soluble species (as $SiO(OH)_3^-$) is at the traces level at this pH.[32,45] Equal volumes of fd-PEG-CR 0.04 mg/mL (2.4×10^{-9} M) and 10^{-3} M silicic acid were mixed. The solution was placed at 4 °C and slowly stirred for 24 h. The final dispersion was dialyzed against distilled water to remove any molecular byproducts and stored at 4 °C.

Mineralization with TiO_2. The precursor used is the water-soluble Titanium(IV) bis (ammonium lactate) dihydroxide (TiBALDH). Equal volumes of fd-PEG-CR 0.04 mg/mL (2.4×10^{-9} M) and TiBALDH 10^{-3} M in water were mixed. The solution was placed at 4 °C and slowly stirred for 24 h. The solution was then diluted 10 times with distilled water and stirred slowly for 3 days. For purification, the final dispersion was dialyzed against distilled water and stored at 4 °C.

Sample Characterization. For the TEM observations, a diluted (by a factor 10) virus solution (8×10^{-3} mg/mL or 4.9×10^{-10} mol/L) was deposited onto freshly glow-discharged 200-mesh Formvar/carbon-coated grids (purchased from Agar) and allowed to settle for 1 min. Grids were then blotted and observed with a Hitachi H-600

dx.doi.org/10.1021/la401170m | *Langmuir* 2013, 29, 8010−8016

microscope operating at 75 kV. Images are recorded with an AMT CCD camera type DVC.

The cryoTEM experiments have been done on the same diluted solutions. The samples were deposited on cryoTEM grids (R2/2 Quantifoil Jena grids) which were surface plasma treated before the vitrification in liquid ethane. The cryoTEM observations were performed on a FEI Technai F20 TEM equipped with a FEG and operating at 200 kV.

The energy dispersive X-ray spectra were acquired on a JEOL high resolution TEM.

The UV−visible spectroscopy experiments were performed on a Unicam UV/vis spectrometer.

RESULTS AND DISCUSSION

Following the processes described in the Experimental Section, individual hybrid rod-like particles virus/SiO_2 and virus/TiO_2 are obtained (Figure 2A,B). The energy dispersive X-ray (EDX) spectra confirm that the electron dense layers observed in transmission electron microscopy (TEM) pictures are SiO_2 and TiO_2, respectively. On these two TEM pictures, a high number of hybrid particles is observed. These particles are not only very well-dispersed (no aggregation is observed on the TEM grids) but also a high quantity of mineralized rods is achieved. Keeping in mind the necessity to produce large amount of particles for potential applications, we have checked that a scaling up by a factor 100 still works (running the experiment with 500 mL solution instead of 5 mL). One of the most remarkable points is the reliability of our process, allowing for the reproducibility of the results in terms of monodispersity and lack of aggregation of the hybrid colloids whatever the inorganic salts, SiO_2 or TiO_2.

In Figure 3, the hybrid rod-like particles are observed in their aqueous environment by electron microscopy at cryogenic temperatures (cryoTEM). This technique allows for freezing the samples in their aqueous stage and so getting rid of the drying effects which can induce aggregation or influence the mineralization probed by usual TEM. We note that the mineral layer is not completely homogeneous but seems to be formed by 1−2 nm nanoparticles aggregated at the virus surface. The concentration of these particles seems to be high enough to fully cover the viral surface in the case of SiO_2 but is much more dispersed for TiO_2. In both cases, the mean thickness of the deposited mineral layer is mainly constant along the whole length of a given virus, and only slightly differ from virus to another one (see the SI for quantitative values of the polydispersity in length and diameter). As usually observed in other mineralization processes, this uniform thickness of the inorganic layer probably stems from a macroscopic electrostatic neutralization of the hybrid system. For SiO_2, the mineralization reaction generally leads to a slightly negatively charged silica deposit due to unreacted silanol groups which counterbalance the cationic template charge until electrostatic neutralization is reached.[7,46] The chemistry of TiBALDH precursor is less known than TEOS, but similar electrostatic effects are expected. Both the size of the formed nanoparticles and the references published in literature about the Ti-BALDH salt used at ambient temperature[33−43] suggest that the TiO_2 covering the virus is in an amorphous state.

To achieve the formation of these highly reliable, monodisperse in size and well-dispersed hybrid rod-like particles, all the three chemical steps described previously are necessary; i.e. the steric stabilization by hydrophilic polymers, the charge surface inversion and finally the mineralization. Figure 4 shows different control experiments which prove the necessity of each step. The importance of the PEGylation is illustrated in Figure 4A,D, where the TEM pictures correspond to the mineralization of positively charged viruses (after the charge inversion step) but without the initial steric stabilization by polymer grafting. Despite similar concentrations, the viruses without polymer stabilization aggregate during the mineralization process, forming thus bundles and fibers for both TiO_2 and SiO_2 (Figure 4A,D, respectively). This is consistent with previous works showing the formation of silica/virus fibers in more concentrated conditions.[17,23] If the PEGylation step is crucial to maintain the colloidal stability of the particles, the mineralization only takes place if some electrostatic attraction exists between the viral template and the inorganic salt as demonstrated in Figure 4B. Indeed, if both the viruses and the

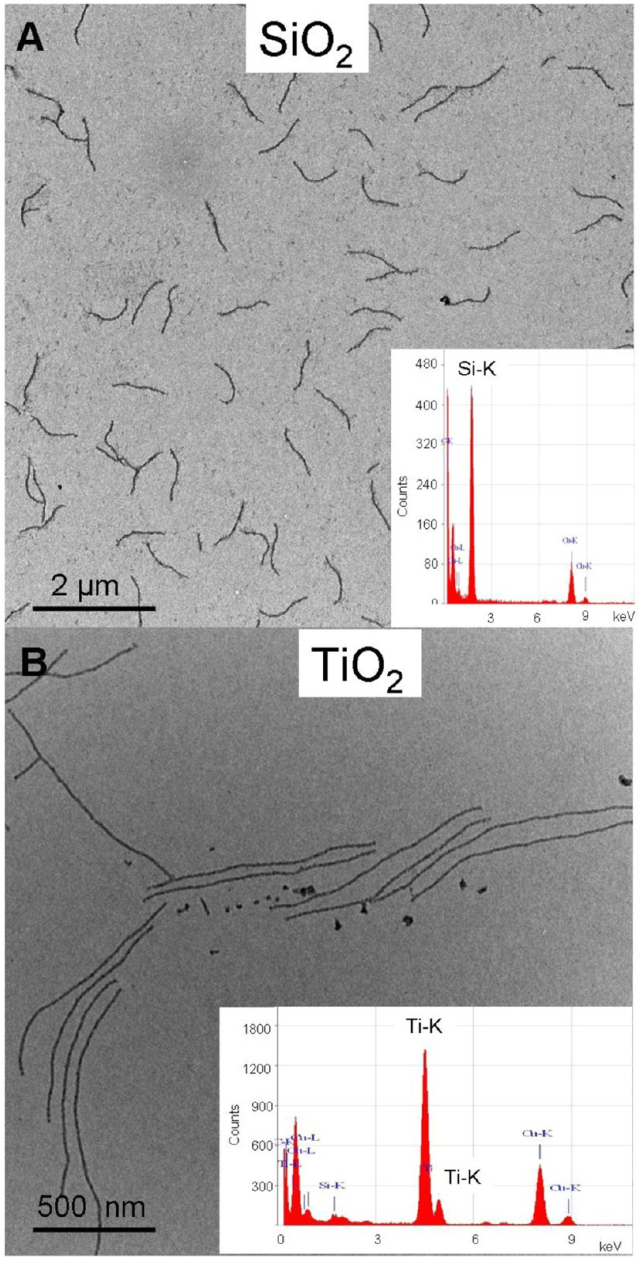

Figure 2. (A) Hybrid virus/SiO_2 and (B) virus/TiO_2 rod-like particles. TEM images and energy dispersive X-ray analysis confirming the presence of SiO_2 and TiO_2 on the viral rod-like particles respectively. The high contrast of the particles is induced by the presence of the mineral shell on the viruses.

dx.doi.org/10.1021/la401170m | Langmuir 2013, 29, 8010−8016

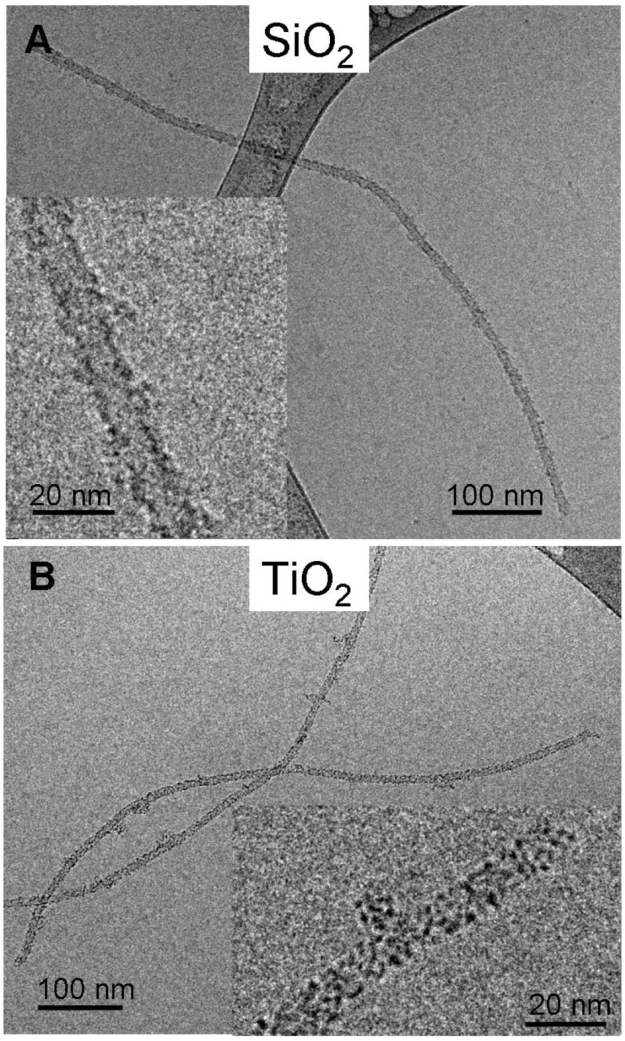

Figure 3. CryoTEM images. (A) Hybrid virus/SiO_2 particles and (B) hybrid virus/TiO_2 particles. These images demonstrate the presence of a thin layer (~2 nm) of SiO_2 on the virus forming a core−shell like structure and the presence of TiO_2 nanoparticles decorating the surface of the viruses.

mineral precursors are negatively charged, no specific mineral deposition is observed at the virus surface (Figure 4B) proving the importance of the virus charge inversion in the mineralization process. For SiO_2 deposition, we have evidenced a specific role of the PEG polymer and more specifically of the polymer grafting density in the silicification process (Figure 4E,F). The cryoTEM images in Figure 4E,F show that for a PEG density of 150 PEG/virus the mineralization is catalyzed by the virus surface, whereas for a concentration of polymers corresponding to 350 PEG/virus the silica deposition is both less dense and heterogeneous and forms a large layer (10−20 nm) made of 1−2 nm silica particles. In this case, the PEG polymers probably play the role of silica condensation catalyzers. This suggestion is reinforced by previous works showing PEG mediated silica formation. It has been evidenced that a cooperative effect exists between the polymers and the silicic acid molecules, forming from 1 to 5 nm diameter SiO_2 nanospheres wrapped around PEG molecules.[47−50] In the presence of silicic acid and PEG, two reactions are in balance:

$$\mathrm{Si{-}(OH)_4 + Si{-}(OH)_4 \rightarrow 2SiO_2 + 4H_2O} \quad (1)$$

$$\mathrm{Si{-}(OH)_4 + HO{-}(CH_2CH_2O)_nH \rightarrow (HO)_3 - Si - O - (CH_2CH_2O)_nH + H_2O} \quad (2)$$

At the surface of the virus, reaction 1 is favored both by the amino groups and the local basic pH induced by the positive charges. In bulk, this competition is driven by the PEG concentration. Indeed, we checked that this cooperative effect only appears for a concentration of PEG above 10^{-3} M (experiments performed with prehydrolyzed TEOS at 10^{-3} M). This value has to be compared to the concentration of the PEG at the virus surface. If we assume that 150 polymers are confined in a volume of two radii of gyration, R_g, around the virus (with R_g = 7 nm for PEG 20 000 g/mol in coil conformation[51]), this gives a polymer concentration of about 10^{-3} M. If this calculation is certainly naive, it seems nevertheless to account for the balance between the two chemical reactions occurring in the close polymer environment. For the lowest polymer concentration of 150 PEG/virus, the mineralization mainly occurs at the surface of the virus, accounting for the homogeneous general aspect of the hybrid particles (Figure 4E). For the high PEG concentration of 350 PEG/virus, the virus surface is less accessible for the silica precursors and the reaction 2 prevails on the PEG chains. This explains the aggregation of the small silica particles around the virus forming a heterogeneous and nondense surface (Figure 4F). Therefore, we show that the degree of PEGylation (number of PEG/virus) of the template is a crucial parameter to monitor, with a balance between the efficiency of the steric stabilization of the particles and a limited reaction of the polymers with the mineral precursors.

If the importance of both the steric colloidal stability by polymer grafting and the virus charge inversion have been demonstrated, we have also to quantify if these two chemical steps before the mineralization process itself do not hinder large amount production of hybrid elongated particles, i.e., if the associated yield is high enough. For this purpose, the virus concentration was determined for the different chemical steps by UV spectrometry. The results are given in Figure 4C, and show that the limiting step (with a corresponding yield of about 64%) is the charge inversion for which some viruses are lost due to formation of aggregates (removed afterward by centrifugation). Because of the contribution in optical absorption of the mineral part of the hybrid viruses, the yield of the mineralization reaction itself can hardly be evaluated. However, we stress that no aggregation is observed directly by eyes or on the TEM grids, considering therefore that virus losses can be neglected during the mineralization reaction. It results in a general yield higher than 50%, which allows for large scale production of hybrid particles.

In conclusion, we describe a novel mineralization route based on the steric stabilization of the organic template by PEGylation. Large aspect ratio, highly monodisperse, and well-dispersed hybrid rod-like particles are obtained on a large scale via a direct chemical approach. A mechanism of the morphosynthesis based on the balance between the degree of PEGylation and the surface mineralization is proposed for the formation of these hybrid particles. The validity of such an approach has been demonstrated with the use of two important inorganic precursors: silica and titanium dioxide. This proof of principle to get high amounts of well-dispersed individual mineralized rod-like particles opens the way toward self-

dx.doi.org/10.1021/la401170m | *Langmuir* 2013, 29, 8010−8016

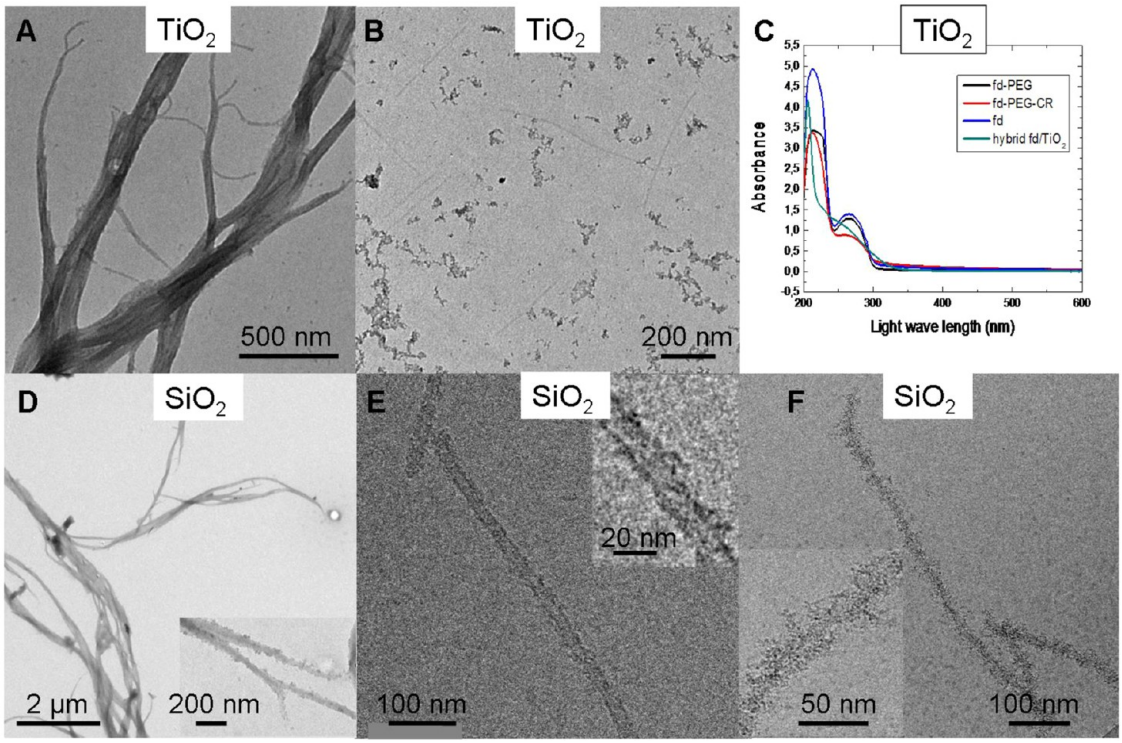

Figure 4. Control experiments for TiO_2 (A–C) and SiO_2 (D–F) mineralization. (A) Mineralization of the viruses with a surfacic charge inversion but no steric repulsion by PEGylation, leading to bundle and fiber formation. (B) No mineralization occurred for viruses after PEGylation but without surface charge inversion. Note the bare viruses in between the mineral aggregates. (C) UV–visible spectra for the determination of the fd virus concentration measured during the three steps of mineralization. This indicates some loss of viruses during the charge inversion due to some aggregation. (D) idem to (A), but for SiO_2. (E) and (F) CryoTEM images of fd-PEG-CR/SiO_2 nanorods with a density of grafted polymers on the virus surface of (E) 150 PEG/virus and F) 350 PEG/virus respectively.

organized mesophases formed by monodisperse inorganic elongated nanoparticles.

■ ASSOCIATED CONTENT

Supporting Information

Additional materials as mentioned in the text. This material is available free of charge via the Internet at http://pubs.acs.org.

■ AUTHOR INFORMATION

Corresponding Author

*E-mail: grelet@crpp-bordeaux.cnrs.fr.

Present Address

†E-mail: e.pouget@iecb.u-bordeaux.fr CBMN/IECB, 2 rue Robert Escarpit, F-33600 Pessac, France.

Author Contributions

The manuscript was written through contributions of all authors. All authors have given approval to the final version of the manuscript.

Notes

The authors declare no competing financial interest.

■ ACKNOWLEDGMENTS

We would like to thank Elisabeth Sellier (CREMEM, Université Bordeaux) for the EDX experiments, Pr. Alain Brisson and Sisareuth Tan (CBMN CNRS/Université Bordeaux) for the cryoTEM observations, Annie Février (CRPP) for her help with the virus growth, and Alexis de la Cotte for preliminary experiments. This work was funded by ANR grants.

■ REFERENCES

(1) Xia, Y.; Peidong, Y.; Sun, Y.; Wu, Y.; Mayers, B.; Gates, B.; Yin, Y.; Kim, F.; Yan, H. One-dimensional nanostructures: synthesis, characterization and applications. *Adv. Mater.* **2003**, *15*, 353.

(2) Mann, S. Self-assembly and transformation of hybrid nano-objects and nanostructures under equilibrium and non-equilibrium conditions. *Nat. Mater.* **2009**, *8*, 781.

(3) Shimizu, T.; Masuda, M.; Minamikawa, H. Supramolecular nanotube architectures based on amphiphilic molecules. *Chem. Rev.* **2005**, *105*, 1401.

(4) Rahman, I. A.; Padavettan, V. Synthesis of silica nanoparticles by sol-gel: size-dependent properties, surface modification and applications in silica-polymer nanocomposites. *J. Nanomater.* **2012**, article ID 132424

(5) Shenton, W.; Douglas, T.; Young, M.; Stubbs, G.; Mann, S. Inorganic/organic nanotube composites from template mineralization of Tobacco Mosaic Virus. *Adv. Mater.* **1999**, *11* (3), 253.

(6) Cozzoli, P. D.; Kornowski, A.; Weller, H. Low-temperature synthesis of soluble and processable organic-capped anatase TiO_2 nanorods. *J. Am. Chem. Soc.* **2003**, *125*, 14539.

(7) Pouget, E.; Dujardin, E.; Cavalier, A.; Moreac, A.; Valery, C.; Marchi-Artzner, V.; Weiss, T.; Renault, A.; Paternostre, M.; Artzner, F. Hierarchical architectures by synergy between dynamical template self-assembly and biomineralization. *Nat. Mater.* **2007**, *6*, 434.

(8) Pouget, E. M.; Bomans, P. H. H.; Dey, A.; Frederik, P. M.; de With, G.; Sommerdijk, N. A. J. M. The development of morphology and structure in hexagonal vaterite. *J. Am. Chem. Soc.* **2010**, *132*, 11560.

(9) Tomczak, M. M.; Glawe, D. D.; Drummu, L. F.; Lawrence, C. G.; Stone, M. O.; Perry, C. C.; Pochan, D. J.; Deming, T. J.; Naik, R. R. Polypeptide-templated synthesis of hexagonal silica platelets. *J. Am. Chem. Soc.* **2005**, *127*, 12577.

(10) Delclos, T.; Aimé, C.; Pouget, E.; Brizard, A.; Huc, I.; Delville, M. H.; Oda, R. Individualized silica nanohelices and nanotubes: tuning inorganic nanostructures using lipidic self-assemblies. *Nano Lett.* **2008**, *8*, 1929.
(11) van Blaaderen, A. Colloids get complex. *Nature* **2006**, *439*, 545.
(12) Glotzer, S. C.; Solomon, M. J. Anisotropy of building blocks and their assembly into complex structures. *Nat. Mater.* **2007**, *6*, 557.
(13) Jana, N. R.; Gearheart, L.; Murphy, C. J. Wet chemical synthesis of high aspect ratio cylindrical gold nanorods. *J. Phys. Chem. B* **2001**, *105*, 4065.
(14) Dickerson, M. B.; Sandhage, K. H.; Naik, R. R. Protein- and Peptide-Directed Syntheses of Inorganic Materials. *Chem. Rev.* **2008**, *108*, 4935.
(15) Sotiropoulou, S.; Sierra-Sastre, Y.; Mark, S. S.; Catt, C. A. Biotemplated Nanostructured Materials. *Chem. Mater.* **2008**, *20*, 821.
(16) Dujardin, E.; Peet, C.; Stubbs, G.; Culver, J. N.; Mann, S. Organization of Metallic Nanoparticles Using Tobacco Mosaic Virus Templates. *Nano Lett.* **2003**, *3*, 413.
(17) Grelet, E.; Moreno, A.; Backov, R. Hybrid Macroscopic Fibers from the Synergistic Assembly Between Silica and Filamentous Viruses. *Langmuir* **2011**, *27*, 4334.
(18) Zhang, Z.; Buitenhuis, J. Synthesis of Uniform Silica Rods, Curved Silica Wires, and Silica Bundles Using Filamentous fd Virus as a Template. *Small* **2007**, *3*, 424.
(19) Fowler, C. E.; Shenton, W.; Stubbs, G.; Mann, S. Tobacco Mosaic Virus Liquid Crystals as Templates for the Interior Design of Silica Mesophases and Nanoparticles. *Adv. Mater.* **2001**, *16*, 1266.
(20) Mao, C.; Solis, D. J.; Reiss, B. D.; Kottmann, S. T.; Sweeney, R. Y.; Hayhurst, A.; Georgiou, G.; Iverson, B.; Belcher, A. M. Virus-Based Toolkit for the Directed Synthesis of Magnetic and Semiconducting Nanowires. *Science* **2004**, *303*, 213.
(21) Huang, Y.; Chiang, C. Y.; Lee, S. K.; Gao, Y.; Hu, E. L.; De Yoreo, J.; Belcher, A. M. Programmable Assembly of Nanoarchitectures Using Genetically Engineered Viruses. *Nano Lett.* **2005**, *5*, 1429.
(22) Nam, K. T.; Lee, Y. J.; Krauland, E. M.; Kottmann, S. Y.; Belcher, A. M. Peptide-Mediated Reduction of Silver Ions on Engineered Biological Scaffolds. *ACS Nano* **2008**, *2*, 1480.
(23) Mao, C.; Wang, F.; Cao, B. Controlling Nanostructures of Mesoporous Silica Fibers by Supramolecular Assembly of Genetically Modifiable Bacteriophages. *Angew. Chem., Int. Ed.* **2012**, *51*, 6411.
(24) Kuijk, A.; van Blaaderen, A.; Imhof, A. Synthesis of Monodisperse, Rodlike Silica Colloids with Tunable Aspect Ratio. *J. Am. Chem. Soc.* **2011**, *133*, 2346.
(25) Sambrook, J.; Russell, D. W. *Molecular Cloning*, 3rd ed.; Cold Spring Harbor Laboratory Press: New York, 2001; Chapter 3.
(26) Marvin, D. A. Filamentous phage structure, infection and assembly. *Curr. Opin. Struct. Biol.* **1998**, *8*, 150.
(27) Zimmermann, K.; Hagedorn, H.; Heucks, C. C.; Hinrichsen, M.; Ludwig, H. The Ionic Properties of the Filamentous Bacteriophages Pfl and fd. *J. Biol. Chem.* **1986**, *261*, 1653.
(28) Zhang, Z.; Buitenhuis, J.; Cukkemane, A.; Brocker, M.; Bott, M.; Dhont, J. K. G. Charge Reversal of the Rodlike Colloidal fd Virus through Surface Chemical Modification. *Langmuir* **2010**, *26*, 10593.
(29) Brutchey, R. L.; Morse, D. E. Silicatein and the translation of its molecular mechanism of biosilicification into low temperature nanomaterial synthesis. *Chem. Rev.* **2008**, *108*, 4915.
(30) Mizatuni, T.; Nagase, H.; Fujiwara, N.; Ogoshi, H. Silicic Acid Polymerization Catalyzed by Amines and Polyamines. *Bull. Chem. Soc. Jpn.* **1998**, *71*, 2017.
(31) Israelachvili, J. *Intramolecular and Surface Forces*, 2nd ed.; Academic Press: San Diego, 1992.
(32) Jolivet, J. P.; Livage, J.; Henry, M. *Metal Oxide Chemistry and Synthesis: From Solution to Oxide*; John Wiley & Sons Ltd.: New York, 2000.
(33) Sumerel, J. L.; Yang, W.; Kisailus, D.; Weaver, J. C.; Choi, J. H.; Morse, D. E. Biocatalytically Templated Synthesis of Titanium Dioxide. *Chem. Mater.* **2003**, *15*, 4804.
(34) Kakihana, M.; Kobayashi, M.; Tomita, K.; Petrykin, V. Application of Water-Soluble Titanium Complexes as Precursors for Synthesis of Titanium-Containing Oxides via Aqueous Solution Processes. *Bull. Chem. Soc. Jpn.* **2010**, *83*, 1285.
(35) Smith, G. P.; Baustian, K. J.; Ackerson, C. J.; Feldheim, D. L. Metal oxide formation by serine and cysteine proteases. *J. Mater. Chem.* **2009**, *19*, 8299.
(36) Kroger, N.; Dickerson, M. B.; Ahmad, G.; Cai, Y.; Haluska, M. S.; Sandhage, K. H.; Poulsen, N.; Sheppard, V. C. Bioenabled Synthesis of Rutile (TiO2) at Ambient Temperature and Neutral pH. *Angew. Chem., Int. Ed.* **2006**, *45*, 7239.
(37) Kharlampieva, E.; Tsukruk, T.; Slocik, J. M.; Ko, H.; Poulsen, N.; Naik, R. R.; Kroger, N.; Tsukruk, V. V Bioenabled Surface-Mediated Growth of Titania Nanoparticles. *Adv. Mater.* **2008**, *20*, 3274.
(38) Fang, Y.; Wu, Q.; Dickerson, M. B.; Cai, Y.; Shian, S.; Berrigan, J. D.; Poulsen, N.; Kroger, N.; Sandhage, K. H. Protein-Mediated Layer-by-Layer Syntheses of Freestanding Microscale Titania Structures with Biologically Assembled 3-D Morphologies. *Chem. Mater.* **2009**, *21*, 5704.
(39) Cole, K. E.; Ortiz, A. N.; Schoonen, M. A.; Valentine, A. M. Peptide- and Long-Chain Polyamine- Induced Synthesis of Microand Nanostructured Titanium Phosphate and Protein Encapsulation. *Chem. Mater.* **2006**, *18*, 4592.
(40) Jiang, Y. Biomimetic synthesis of titania nanoparticles induced by protamine. *Dalton Trans.* **2008**, 4165.
(41) Cole, K. E.; Valentine, A. M. Spermidine and Spermine Catalyze the Formation of Nanostructured Titanium Oxide. *Biomacromolecules* **2007**, *8*, 1641.
(42) Sewell, S. L.; Wright, D. W. Biomimetic synthesis of titanium dioxide utilizing the R5 peptide derived from cylindrotheca fusiformis. *Chem. Mater.* **2006**, *18*, 3108.
(43) Dickerson, M. B.; Jones, S. E.; Cai, Y.; Ahmad, G.; Naik, R. R.; Kroger, N.; Sandhage, K. H. Identification and Design of Peptides for the Rapid, High-Yield Formation of Nanoparticulate TiO2 from Aqueous Solutions at Room Temperature. *Chem. Mater.* **2008**, *20*, 1578.
(44) Dogic, Z.; Fraden, S. Development of model colloidal liquid crystals and the kinetics of the isotropic smectic transition. *Trans. R. Soc. London, Ser. A* **2001**, *359*, 997.
(45) Tarutani, T. Polymerization of silicic acid. *Anal. Sci.* **1989**, *5*, 245.
(46) Brinker, C. J. ; Scherer, G. W. *Sol−Gel Science. The Physics and Chemistry of Sol−Gel Processing*; Academic Press: New York, 1990.
(47) Sun, Q.; Beelen, T. P. M.; van Santen, R. A.; Hazelaar, S.; Vrieling, E. G.; Gieskes, W. W. C. PEG-Mediated Silica Pore Formation Monitored in Situ by USAXS and SAXS: Systems with Properties Resembling Diatomaceous Silica. *J. Phys. Chem. B* **2002**, *106*, 11539.
(48) Lesot, P.; Chapuis, S.; Bayle, J. P.; Rault, J.; Lafontaine, E.; Camperod, A.; Judeinstein, P. Structural−dynamical relationship in silica PEG hybrid gels. *J. Mater. Chem.* **1998**, *8*, 147.
(49) Sierra, L.; Guth, J. L. Synthesis of mesoporous silica with tunable pore size from sodium silicate solutions and a polyethylene oxide surfactant. *Microporous Mesoporous Mater.* **1999**, *27*, 243.
(50) Wong, K.; Lixon, P.; Lafuma, F.; Lindner, P.; Aguerre-Charriol, O.; Cabane, B. Intermediate structures in equilibrium flocculation. *J. Colloid Interface Sci.* **1992**, *153*, 55.
(51) Devanand, K.; Selser, J. C. Asymptotic Behavior and Long-Range Interactions in Aqueous Solutions of Poly(ethy1ene oxide). *Macromolecules* **1991**, *24*, 5943.

Supporting Information

Dispersions of Monodisperse Hybrid Rod-Like Particles by Mineralization of Filamentous Viruses

Emilie Pouget and Eric Grelet*

CNRS & Université de Bordeaux, Centre de Recherche Paul-Pascal,

115 Avenue Schweitzer, F-33600 Pessac, France

* Corresponding author: grelet@crpp-bordeaux.cnrs.fr

1. Grafting of the ethylenediamine on the carboxylic groups of the virus surface

The grafting of the ethylenediamine (EDA) on the carboxylic groups of the virus surface is catalyzed by 1-ethyl-3-(3-dimethylaminopropyl)carbodiimide hydrochloride (EDAC). An amide bond is formed and the negative charge of the carboxylic group is reversed into a positive one by the amine terminated group. It results in a general positive surfacic charge of the modified virus at physiological pH.

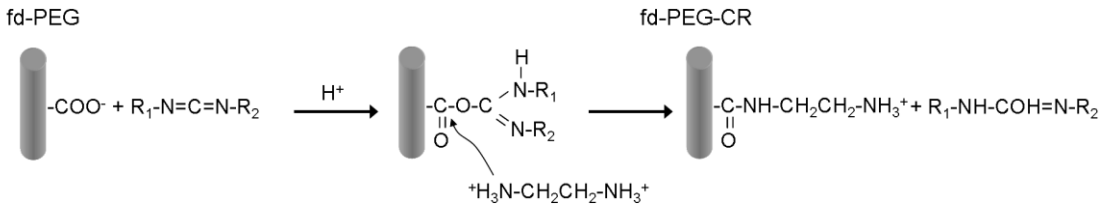

2. Contour length and diameter distributions of the mineralized rod-like particles

From the TEM images, we obtained a distribution of the contour lengths, L, and the diameters, D, of the hybrid rods synthesized. The mean distribution peaks have been fitted by a Gaussian function (red lines) to provide the average values and the standard deviations.

Contour lengths:

Virus / TiO_2

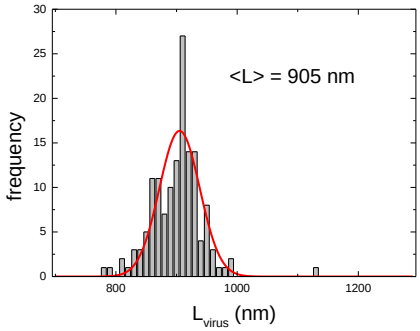

Virus / SiO_2

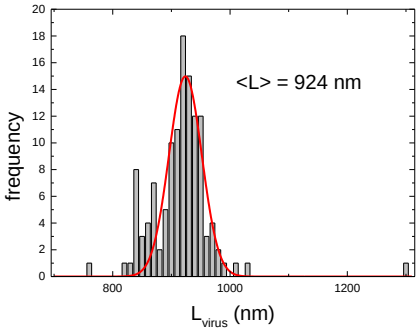

Diameters:

Virus / TiO_2

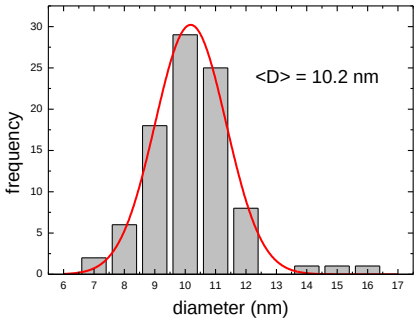

Virus / SiO_2 *150 PEG/virus*

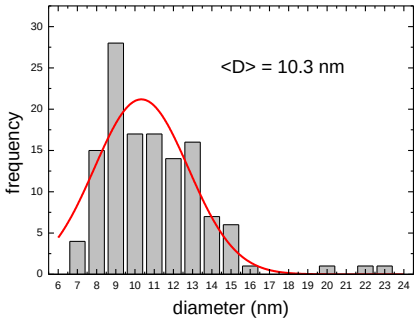

Virus / SiO_2 *300 PEG/virus*

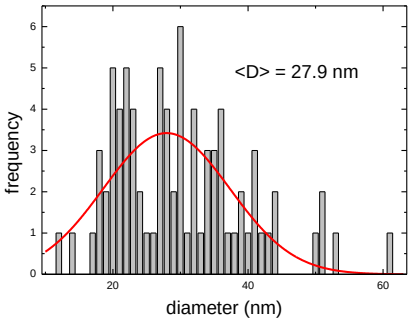

The polydispersity, σ, is defined by the relative standard deviation of the Gaussian distribution : $\sigma_L=((<L^2>-<L>^2))^{1/2}/<L>$, where the brackets indicate a statistical average.

The following polydispersities in length (σ_L) and diameter (σ_D) are then obtained:

Virus / TiO_2: σ_L = 3.5%

σ_D = 11.2%

Virus / SiO_2: σ_L = 2.8%

σ_D = 23.3% for 150 PEG/virus

σ_D = 32% for 300 PEG/virus